

# Exercise-responsive phosphoproteins in the heart.

Hongbo Guo<sup>1</sup>, Ruth Isserlin<sup>1</sup>, Andrew Emili<sup>1\*</sup> and Jatin G Burniston<sup>2†</sup>

<sup>1</sup>Donnelly Centre for Cellular & Biomolecular Research, Department of Molecular Genetics, University of Toronto, Ontario, M5S 3E1, Canada. <sup>2</sup>Research Institute for Sport & Exercise Sciences, Liverpool John Moores University, Liverpool, L3 3AF, United Kingdom.

\*Address for Correspondence: Professor Andrew Emili  
Donnelly Centre for Cellular & Biomolecular Research,  
University of Toronto,  
160 College St,  
Toronto ON, M5S 3E1,  
Canada.  
Tel: +1 416 946 7281  
Email: [andrew.emili@utoronto.ca](mailto:andrew.emili@utoronto.ca)

†Address for Correspondence: Professor Jatin G Burniston  
Research Institute for Sport & Exercise Sciences  
Liverpool John Moores University,  
Tom Reilly Building, Byrom Street,  
Liverpool, L3 3AF,  
United Kingdom.  
Tel: +44 151 904 6265  
Email: [j.burniston@ljmu.ac.uk](mailto:j.burniston@ljmu.ac.uk)

## 29 **Abstract**

30 Endurance exercise improves cardiac performance and affords protection against cardiovascular diseases but  
31 the signalling events that mediate these benefits are largely unexplored. Phosphorylation is an widely studied  
32 post-translational modification involved in intracellular signalling, and to discover novel phosphorylation  
33 events associated with exercise we have profiled the cardiac phosphoproteome response to a standardised  
34 exercise test to peak oxygen uptake (VO<sub>2</sub>peak).

35 Male Wistar rats (346 ± 18 g) were assigned to 3 independent groups (n= 6, in each) that were familiarised  
36 with running on a motorised treadmill within a metabolic chamber. Animals performed a graded exercise test  
37 and were killed either immediately (0 h) after or 3 h after terminating the test at a standardised physiological  
38 end point (i.e. peak oxygen uptake; VO<sub>2</sub>peak). Control rats were killed at a similar time of day to the  
39 exercised animals, to minimise possible circadian effects. Cardiac proteins were digested with trypsin and  
40 phosphopeptides were enriched by selective binding to titanium dioxide (TiO<sub>2</sub>). Phosphopeptides were  
41 analysed by liquid chromatography and high-resolution tandem mass spectrometry, and phosphopeptides were  
42 quantified by MS1 intensities and identified against the UniProt knowledgebase using MaxQuant (data are  
43 available via ProteomeXchange, ID PXD006646).

44 The VO<sub>2</sub>peak of rats in the 0 h and 3 h groups was 66 ± 5 ml•kg<sup>-1</sup>•min<sup>-1</sup> and 69.8 ± 5 ml•kg<sup>-1</sup>•min<sup>-1</sup>,  
45 respectively. Proteome profiling detected 1169 phosphopeptides and one-way ANOVA found 141 significant  
46 (P<0.05 with a false discovery rate of 10 %) differences. Almost all (97 %) of the phosphosites that were  
47 responsive to exercise are annotated in the PhosphoSitePlus database but, importantly, the majority of these  
48 have not previously been associated with the cardiac response to exercise. More than two-thirds of the  
49 exercise-responsive phosphosites were different from those identified in previous phosphoproteome profiling  
50 of the cardiac response to β<sub>1</sub>-adrenergic receptor stimulation. Moreover, we report entirely new  
51 phosphorylation sites on 4 cardiac proteins, including S81 of muscle LIM protein, and identified 7 exercise-  
52 responsive kinases, including myofibrillar protein kinases such as obscurin, titin and the striated-muscle-  
53 specific serine/threonine kinase (SPEG) that may be worthwhile targets for future investigation.

54 **Keywords:**

55 Proteomics; phosphorylation; time-series; cardiac muscle; exercise; maximum oxygen uptake

56

57 **Abbreviations:**

58 Adrenergic receptor (AR), Carbon dioxide production (VCO<sub>2</sub>), Electrospray ionisation (ESI), False discovery

59 rate (FDR), High-energy collision-induced dissociation (HCD), Mass spectrometry (MS), Oxygen uptake

60 (VO<sub>2</sub>), Peak oxygen uptake (VO<sub>2peak</sub>), Tandem mass spectrometry (MS/MS), Serine (S), Titanium dioxide

61 (TiO<sub>2</sub>), Threonine (T), Tyrosine (Y).

62

## 63 **1. Introduction**

64 Exercise has an irrefutable role in preventing heart failure and cardiac diseases, for example acute exercise has  
65 cardio-protective effects similar to ischaemic preconditioning {Frasier 2011} and chronic exercise training  
66 results in physiological cardiac hypertrophy {Bernardo 2016} and a heart phenotype that affords protection  
67 against pathological insults such as ischaemia/reperfusion injury {Powers 2008}. Although the physiological  
68 benefits of exercise are clear, less is known about the molecular mechanisms that underlie these effects. Yet  
69 greater molecular understanding could enable the benefits of exercise to be further optimised or personalised  
70 and could suggest new targets for more effective modes of diagnosis, prevention or rehabilitation of  
71 debilitating cardiac diseases.

72 Previous work has investigated discrete signalling events activated in response to exercise, for example in the  
73 context of acute cardiac preconditioning {Frasier 2011} or adaptive versus maladaptive cardiac  
74 hypertrophy {Bernardo 2016}. The IGF-1 receptor/PI3K (p110 $\alpha$ )/ Akt1 pathway is perhaps the most well-  
75 explored regulatory pathway associated with exercise-induced cardiac hypertrophy but it is unlikely that a  
76 biological phenomenon as complex as cardiac growth is entirely mediated by a single pathway and more often  
77 integrated networks of molecules across multiple pathways are required to achieve physiological adaptations  
78 to environmental stimuli {Bhalla 1999}. Therefore, events outside of the canonical IGF-1R/ PI3K(p110 $\alpha$ )/  
79 Akt1 pathway are likely to also contribute to exercise-induced cardiac adaptations and remain to be  
80 discovered.

81 Vigorous exercise is associated with significant elevations in cardiac work and myocardial contractility which  
82 are driven by the chronotropic and inotropic effects of beta-adrenergic receptor (AR) signalling (sympathetic  
83 drive) as well as local metabolic responses and mechanical strain. In addition to driving acute increases in  
84 cardiac output, the molecular events associated with exercise also instigate adaptive processes that alter the  
85 cardiac proteome {Burniston 2009} and increase the capacity for work (i.e. VO<sub>2</sub>peak). Phosphorylation  
86 networks are recognised widely in the literature and are known to transduce signals involved in the skeletal  
87 muscle response to exercise in humans {Hoffman 2015} but until now the cardiac phosphoproteome response  
88 to exercise has not been reported. Phosphoproteome profiling is a useful approach to discover the pathways  
89 and signalling events involved in physiological processes, and a key advantage of this technique is its non-

90 targeted approach that it is not biased by preconceptions about which pathways or events may be of greatest  
91 importance.

92 Due to the implausibility of sampling human cardiac tissue in the context of exercise physiology, models are  
93 required that simulate exercise prescription in humans while allowing access to the heart for molecular  
94 investigation. The exercise stimulus is a composite of 3 inter-related variables, i.e. exercise intensity, duration  
95 and frequency, and the cardio-protective of exercise is intensity-dependent {Frasier 2011}. Therefore, to  
96 control and standardise exercise intensity we {Burniston 2009} have used indirect calorimetry and an  
97 incremental protocol of exercise on a motorised treadmill to measure peak oxygen uptake ( $VO_{2peak}$ ) of rats  
98 in a manner that is equivalent to best practice in human studies (e.g. {Holloway 2009}). During the  $VO_{2peak}$   
99 test the animal's respiratory gases are monitored and the test is terminated when the animal reaches its peak  
100 aerobic capacity (this intensity of exercise is attainable even by previously sedentary animals). By using this  
101 physiological end-point we minimise the influence of acute stress induced by an unrealistic exercise load.  
102 Such, standardisation is important because differences in exercise capacity exist even within a colony of  
103 animals exposed to identical environmental conditions. Therefore, exposure to the same relative exercise  
104 stimulus represents an optimised model with the best chances of successfully identifying the key regulatory  
105 networks that mediate exercise-induced adaptation.

106

## 107 **2. Methods**

### 108 **2.1. Graded treadmill test of peak oxygen uptake**

109 Experiments were conducted under the British Home Office Animals (Scientific Procedures) Act 1986 and  
110 according to UK Home Office guidelines. Male Wistar rats were bred in-house in a conventional colony and  
111 the environmental conditions controlled at  $20 \pm 2$  °C, 45-50% humidity with a 12-h light (1800-0600) and  
112 dark cycle. Water and food (containing 18.5% protein) were available ad libitum.

113 Exercise sessions were conducted during the animals' dark period. All rats ( $n = 18$ ) completed a 14-day  
114 familiarization procedure encompassing daily bouts (15 min duration) at various belt speeds and inclines on a  
115 motorized treadmill within a metabolic chamber (Columbus Instruments, OH). On the 15th day the  $VO_2$ peak  
116 of animals ( $n = 12$ ) assigned to the exercise groups was measured using an incremental test, as described  
117 previously {Burniston 2009; Burniston 2008}. Briefly, a warm-up (5 min running at  $6 \text{ m} \cdot \text{min}^{-1}$ ,  $0^\circ$  incline)  
118 was completed followed a series of 3 min stages of alternating increases in speed (increments of  $2 \text{ m} \cdot \text{min}^{-1}$ )  
119 and incline (increments of  $5^\circ$ ; maximum incline  $25^\circ$ ). Air pumped ( $2.5 \text{ l} \cdot \text{min}^{-1}$ ) through the chamber was  
120 analysed for concentrations of oxygen and carbon dioxide (Oxymax system; Columbus Instruments, OH;  
121 calibrated to an external standard) and a metal grid at the rear of the treadmill belt, which delivered a  
122 maximum of 3 electric stimuli ( $0.1 \text{ mA}$ ,  $0.3 \text{ s}$  duration), was used to encourage the animals to achieve their  
123  $VO_2$ peak. Independent groups ( $n = 6$ , in each) of animals were killed by cervical dislocation either  
124 immediately ( $0 \text{ h}$ ) after cessation of the exercise test or  $3 \text{ h}$  after completing the exercise test. Hearts were  
125 isolated from the exercised animals and from control rats ( $n = 6$ ) that completed the familiarization training  
126 but did not perform an incremental exercise test. Hearts were rapidly isolated, cleaned and weighed before  
127 being stored at  $-80$  °C. To minimize the influence of circadian differences, control rats were killed at a time of  
128 day coinciding with the incremental exercise test.

129

### 130 **2.2. Sample preparation**

131 Left ventricles were pulverized in liquid nitrogen and an accurately weighed portion ( $100 \text{ mg}$ ) homogenized  
132 on ice in 10 volumes of  $8 \text{ M}$  urea, 4% w/v CHAPS,  $40 \text{ mM}$  Tris base including protease and phosphatase  
133 inhibitor cocktails (Roche Diagnostics, Lewes, UK) at  $4$  °C. After centrifugation at  $20,000 \text{ g}$ ,  $4$  °C for  $45 \text{ min}$

134 the supernatant was decanted and the protein concentration measured using a modified 'microtitre plate'  
135 version of the Bradford assay (Sigma, Poole, Dorset, UK).

136 Aliquots containing 2 mg protein were reduced with 2.5 mM dithiothreitol for 1 h at room temperature then  
137 alkylated with 5 mM iodoacetamide for 45 min in the dark at room temperature. Samples were diluted with 50  
138 mM ammonium bicarbonate to bring the concentration of urea to 1M and sequencing-grade trypsin (Promega)  
139 was added at a substrate to enzyme ratio of 50:1. After 4 h, samples were diluted threefold with 50 mM  
140 ammonium bicarbonate containing additional trypsin, and the digestion was allowed to proceed overnight.  
141 After acidification to a final concentration of 1 % (v/v) formic acid, the peptide solutions were desalted using  
142 disposable Tiptip C18 columns (Glygen) and lyophilized to dryness. Phosphopeptides were selectively  
143 enriched by binding to titanium dioxide (TiO<sub>2</sub>)-coated magnetic beads (Pierce) according to the  
144 manufacturer's instructions, as described in previously {Guo 2013}. Briefly, peptides were resuspended in  
145 200 µL 80 % acetonitrile, 2 % formic acid and incubated for 1 min with 10 µL of slurry containing TiO<sub>2</sub>  
146 magnetic beads. Unbound peptides and supernatant were decanted and the beads were washed three times  
147 with 200 µL binding buffer (supplied with the kit). After final decanting, the beads were incubated for 10 min  
148 with 30 µL elution buffer and the eluate was carefully removed and dried prior to mass spectrometry analysis.

149

### 150 2.3. Mass spectrometry analysis

151 Tryptic peptide mixtures were analysed by nano-scale high-performance liquid chromatography (Proxeon  
152 EASY-Nano system) and online nano electrospray ionization (ESI) tandem mass spectrometry (LTQ-Orbitrap  
153 Velos mass spectrometer; Thermo Fisher Scientific). Samples were loaded in aqueous 0.1% (v/v) formic acid  
154 via a trap column constructed from 25 mm of 75 µm i.d. silica capillary packed with 5 µm Luna C18  
155 stationary phase (Phenomenex). The analytical column was constructed in a 100 mm × 75 µm i.d. silica  
156 capillary packed with 3 µm Luna C18 stationary phase. Mobile phase A, consisted of 5 % acetonitrile and 0.1  
157 % formic acid, and organic phase B contained 95 % acetonitrile and 0.1 % formic acid. Reverse phase  
158 separation was performed over 120 min at a flow rate of 300 nL/min, rising to 6 % B in 1 min then from 6 %  
159 to 24 % B over 89 min followed by a 16 min gradient to 100 % B, which was held for 5 min prior to re-  
160 equilibration to 0 % B over 9 min. Eluted peptides were sprayed directly in to an LTQ-Orbitrap Velos mass

161 spectrometer using a nanospray ion source (Proxeon). Tandem mass spectrometry (MS/MS) was performed  
162 using high-energy collision-induced disassociation (HCD) and 10 MS/MS data-dependent scans (7,500  
163 resolution) were acquired in centroid mode alongside each profile mode full-scan mass spectra (30,000  
164 resolution), as reported previously {Guo 2013}. The automatic gain control (AGC) for MS scans was  $1 \times 10^6$   
165 ions with a maximum fill time of 250 ms. The AGC for MS/MS scans was  $3 \times 10^4$ , with 150 ms maximum  
166 injection time, 0.1 ms activation time, and 40% normalized collision energy. To avoid repeated selection of  
167 peptides for MS/MS a dynamic exclusion list was enabled to exclude a maximum of 500 ions over 30 s.

168

## 169 2.4. Protein identification

170 Data files (RAW format) were searched using the standard workflow of MaxQuant (version 1.3.0.5;  
171 <http://maxquant.org/>) against a non-redundant rat protein sequence FASTA file from the UniProt/ SwissProt  
172 database modified to contain porcine trypsin sequences. The search parameters allowed 2 missed cleavages,  
173 carbamidomethylation of cysteine (fixed) and variable oxidation of methionine, protein N-terminal acetylation  
174 and phosphorylation of STY residues. Precursor ion tolerances were 20 ppm for first search and 6 ppm for a  
175 second search. The MS/MS peaks were de-isotoped and searched using a 20 ppm mass tolerance. A stringent  
176 false discovery rate threshold of 1 % was used to filter candidate peptide, protein, and phosphosite  
177 identifications. The mass spectrometry proteomics data have been deposited to the ProteomeXchange  
178 Consortium via the PRIDE {Vizcaíno 2016} partner repository with the dataset identifier PXD006646.

179

## 180 2.5. Bioinformatic Analysis

181 Raw intensities were extracted from the MaxQuant evidence files using an in-house Perl script. Briefly, the  
182 intensities from each biological replicate were collapsed to a specific phosphorylation site as opposed to a  
183 specific peptide. The residue number (e.g. S224 – phosphorylation on the 224<sup>th</sup> residue (serine) of the protein)  
184 was extracted from the FASTA file used for the original MaxQuant protein search and in any given biological  
185 replicate every intensity that can attributed to S224 is summed. If multiple phosphorylations exist on a peptide  
186 then the intensities are counted only for the multi-phosphorylation, i.e. single, double and multi  
187 phosphorylation become different entities and are scored accordingly. Phospho expression sets were



188 normalized in R using quantile normalization in the limma package. Each modification was scored for  
189 differential expression using one-way analysis of variance (ANOVA) across the 3 different time points  
190 (control, 0 h and 3 h) complemented by independent t-tests of each pairwise comparison (i.e. 0 h vs control,  
191 and 3 h vs control). The false discovery rate (FDR) was assessed by calculating q values {Storey 2003} from  
192 the p value distribution of the ANOVA outputs. Protein identifiers associated with statistically significant  
193 ( $P < 0.05$ , FDR  $< 10\%$ ) exercise-responsive phosphopeptides were uploaded to David GO  
194 (<https://david.ncifcrf.gov>) {Huang 2009; Huang 2009b} for functional annotation and association to KEGG  
195 pathways. Hierarchical clustering was performed using the Graphical Proteomics data Explorer (GProX)  
196 {Rigbolt 2011} and protein interactions were investigated using bibliometric mining in the search tool for the  
197 retrieval of interacting genes/proteins (STRING; <http://string-db.org/>) {Franceschini 2013}.

198

## 199 2.6. Western blot analyses

200 Immuno-detection of selected targets was performed using previously described {Burniston 2014} methods.  
201 Briefly, samples containing 50  $\mu\text{g}$  protein were resolved by denaturing gel electrophoresis and transferred on  
202 to polyvinylidene difluoride membranes. Non-specific protein interactions were blocked by incubating the  
203 membranes with 5 % non-fat dry milk in 20 mM Tris, 150 mM NaCl, and 0.1% Tween 20, pH 7.6 (TBS-T)  
204 for 1 hr at room temperature. Membranes were then washed in TBS-T and incubated overnight with TBS-T  
205 containing 5 % BSA and primary antibodies specific for: p38 mitogen activated protein kinase (p38 MAPK;  
206 9212 Cell Signalling Technology; 1:1,000 dilution) and phosphorylated (T180/Y182) p38 MAPK (9211 Cell  
207 Signalling Technology; 1:1,000 dilution) or alpha B crystallin (CRYAB; ab13497 Abcam; 1:10,000 dilution)  
208 and phosphorylated (S59) CRYAB (ab5577 Abcam; 1:5,000 dilution). Serial washes in TBS-T were per-  
209 formed prior to and after incubation with secondary antibodies (goat anti-rabbit IgG; ab205718 Abcam;  
210 1:20,000 dilution) in 5 % BSA in TBS-T for 2 h followed by enhanced chemiluminescence (ECL Prime; GE  
211 Healthcare) and digitization (Gel Doc XRS; Bio-Rad, Hercules, CA) of immuno-reactive protein bands.  
212 Image analysis (Quantity One, version 4.; Bio-Rad) was used to measure the relative abundances of target  
213 proteins. Analysis of phosphorylated and non-phosphorylated species was achieved by stripping (incubation

214 in 62.5 mM Tris, 70 mM SDS, 50 mM  $\beta$ -mercaptoethanol, pH 6.8 at 50 °C for 30 min) and re-probing of  
215 membranes.

216

### 217 3. Results

218 Three independent groups (n= 6, in each) of rats were used to investigate the time course of changes in the  
219 heart phosphoproteome in response to a standardised bout of endurance exercise. The body weight or heart  
220 weight of rats assigned to the control, 0 h and 3 h groups was similar and rats that performed the incremental  
221 exercise test (i.e. 0 h and 3 h groups) had equivalent peak exercise capacities (Table 1). An example of VO<sub>2</sub>  
222 VCO<sub>2</sub> traces recorded during an incremental exercise test is illustrated in Figure 1. The average time to  
223 complete the incremental exercise test was 21 min and the average VO<sub>2peak</sub> of animals in the 0 h and 3 h  
224 groups was  $66 \pm 5 \text{ ml}\cdot\text{kg}^{-1}\cdot\text{min}^{-1}$  and  $69.8 \pm 5 \text{ ml}\cdot\text{kg}^{-1}\cdot\text{min}^{-1}$ , respectively.

225 LC-MS/MS profiled 1,169 phosphopeptides and there were 841 singly phosphorylated peptides were detected  
226 and of these 11 were pY, 90 were pT and 840 were pS. There were also 289 doubly phosphorylated peptides,  
227 30 triply phosphorylated and 10 peptides that had between 4 and 6 phosphorylated residues. One-way  
228 ANOVA found 141 peptide differences at  $P < 0.05$ , the false discovery rate (FDR) calculated from q values  
229 {Storey 2003} was estimated to be 10 %. Volcano plots are illustrated in Figure 2 to highlight post-hoc  
230 analysis of phosphopeptides that differed between the control and 0 h group (Figure 2A) or between control  
231 and 3 h group (Figure 2B). Immediately after cessation of exercise similar numbers of phosphopeptides were  
232 increased and decreased in abundance compared to control. After 3 h recovery (Figure 2B) the majority of  
233 phosphopeptides were more abundant in exercised hearts compared to control.

234 The 141 peptides that significantly differed in response to acute exercise mapped to 97 proteins, i.e. some  
235 proteins had more than one phosphopeptide. Examples of proteins that had multiple phosphorylated peptides  
236 include titin (10 peptides), tensin (5 peptides), Bcl2-interacting death suppressor (5 peptides), alpha-2-HS-  
237 glycoprotein (4 peptides), pyruvate dehydrogenase E1 component subunit alpha (4 peptides) and isoform 2 of  
238 NDRG2 protein (3 peptides).

239 Exercise-responsive phosphopeptides were uploaded to David GO for functional annotation and the top  
240 ranking significant ( $P < 0.05$ ; Fischer with BH correction) KEGG pathways were arrhythmogenic right  
241 ventricular cardiomyopathy, cardiac muscle contraction and adrenergic signalling in cardiomyocytes.

242 Mapping to PhosphoSitePlus (<http://www.phosphosite.org>) found all but 4 (97 %) of the identified  
243 phosphopeptides had previously been reported. The most commonly reported phosphosites matching to  
244 published high-throughput (MS2) data were pyruvate dehydrogenase E1 component subunit alpha  
245 S232&S239, gap junction alpha-1 protein S325& S328, septin-2 S218 and heat shock protein beta-1 S15.  
246 Approximately 28 % (39 of 141) of the exercise-responsive phosphorylation sites were also associated with  
247 low-throughput experimental evidence in PhosphoSitePlus, including p38 mitogen-activated protein kinase  
248 Y182, cardiac phospholamban S16, alpha B-crystallin S59 and cardiac troponin I S23. Western blot analysis of  
249 phosphorylated and non-phosphorylated forms of p38 MAPK and alpha B crystallin (Figure 3) verified  
250 statistically significant differences in the phosphorylation status of these proteins discovered by LC-MS/MS  
251 phosphopeptide profiling.

252 The time-series experimental design was used to provide further associational evidence between  
253 phosphorylation events and the cardiac exercise response. Hierarchical cluster analysis was performed in  
254 GProX to find similarities in the temporal patterns of exercise responsive phosphopeptides (n = 141, P<0.05).  
255 The temporal responses in phosphopeptide abundance organised in to 3 prominent clusters (Figure 4A). Gene  
256 identifiers of exercise responsive phosphoproteins from each cluster were uploaded to STRING and Panels B,  
257 C and D of Figure 4 illustrate interaction networks within each cluster based on literature and database  
258 information, including co-expression, protein-protein interaction and literature mining.

259

## 260 **4. Discussion**

261 The mediators of exercise-induced cardiac adaptation have been less thoroughly investigated than the  
262 mechanisms of pathological cardiac maladaptation, but greater knowledge regarding the physiological  
263 responses of the heart could provide a valuable contrast to data from pathological models. To address this  
264 need, we performed phosphoproteomic profiling to generate new knowledge regarding the cardiac  
265 phosphoproteome response to exercise. To minimise potential mis-identification of phosphorylation events  
266 that may be associated with a supra-physiological cardiac stress rather than the response to physiological  
267 exercise, the oxygen uptake (Figure 1) of each animal was monitored and the exercise test was terminated at a  
268 standardised physiological end point (VO<sub>2</sub>peak). We discovered entirely new phosphorylation sites on 4  
269 cardiac proteins (Table 2), including S81 of muscle LIM protein, and identified 7 exercise-responsive kinases  
270 (Table 3). Almost all (97 %) of the phosphosites that responded significantly to exercise (supplementary Table  
271 S1) were annotated in the PhosphoSitePlus database but, importantly, the majority of these had not previously  
272 been associated with the cardiac response to exercise. Therefore the current data provides a rich source of new  
273 information relating to the potential mediators of exercise-induced cardiac protection.

274 Muscle LIM protein (MLP; also known as cysteine and glycine-rich protein 3) is an essential component of  
275 myogenic differentiation {Arber 1994} and contains 2 LIM domains which facilitate protein-protein  
276 interactions. LIM domain containing proteins are important mediators of signals between the cytoskeleton and  
277 nucleus {Kadmas 2004} and we discovered a new phosphorylation of S81 (significantly greater 3 h after  
278 exercise) which lies within a flexible region between LIM domain 1 (residues 10-61) and LIM domain 2  
279 (residues 120-171) of MLP and is close to a previously reported site (S95) that is phosphorylated during beta-  
280 1 AR stimulation {Lundby 2013}. Other phosphorylation sites of rat MLP include S111 and S153 but  
281 phosphorylation/ de-phosphorylation of these sites has not yet been linked to environmental stimuli or cell  
282 signalling processes. MLP can interact with a number of myogenic factors {Kong 1997} and also proteins at  
283 the myofibril z-disc, including alpha-actinin {Geier 2003}, beta-spectrin {Flick 2000} and the titin capping  
284 protein, telethonin/ TCAP {Knöll 2002}. Translocation of MLP from the sarcomere to the nucleus is  
285 facilitated by a nuclear localisation signal (residues 64-69) and inhibition of MLP nuclear translocation  
286 prevents the protein synthetic response to cyclic strain in cardiomyocytes {Boateng 2009}.

287 We speculate MLP may also be involved in transducing signals in response to exercise in vivo and the novel  
288 S81 phosphorylation reported here may influence the protein-protein interactions and subcellular localisation  
289 of MLP. The amino acid sequence flanking S81 of MLP (Table 1) does not match the linear motifs recognised  
290 by well-defined protein kinases, but our phosphoproteome profiling identified a selection of exercise-  
291 responsive myofibrillar protein kinases (Tables 2 and 3) that could be potential mediators of MLP S81  
292 phosphorylation at the z-disc. Two novel exercise-induced phosphorylation events (Table 2) were discovered  
293 on myofibrillar protein kinases (myosin light chain kinase 3 and obscurin) and may be involved in the  
294 transduction of mechanical signals within the exercised heart. Myosin light chain kinase 3 is responsible for  
295 the phosphorylation of ventricular regulatory myosin light chain, which contributes to the enhancement of  
296 myocardial contractility {Kampourakis 2016} and we report novel S444 phosphorylation of myosin light  
297 chain kinase 3 occurs during vigorous exercise (Cluster 1).

298 Obscurin is also a member of the myosin light chain kinase family along with striated muscle-specific  
299 serine/threonine kinase (SPEG; Table 3) and these kinases are predicted to target similar conserved sites  
300 {Sutter 2004} and may be involved in the hypertrophic response of the heart {Borisov 2006}. In exercised  
301 hearts, we discovered greater phosphorylation of obscurin S2974, which has not previously been reported, and  
302 phosphorylation of SPEG S2410 & S2414 that was reported {Lundby 2013} in phosphoproteome profiling of  
303 the cardiac response to  $\beta$ 1-adrenergic receptor (AR) stimulation. Phosphorylation of SPEG has also recently  
304 been reported {Potts 2017} in phosphoproteome analysis of mouse skeletal muscle submitted to a bout of  
305 maximal isometric contractions. These independent discoveries of SPEG phosphorylation using non-targeted  
306 techniques provide reciprocal verification and further highlight SPEG as an exercise-responsive  
307 phosphoprotein/ kinase of interest for future mechanistic study. Phosphorylation of the giant myofibrillar  
308 protein kinase, titin, was also detected after exercise (Table 3) and each of the titin phosphorylation sites  
309 reported here (Table S1) is also known to be responsive to  $\beta$ 1-AR stimulation. Taken together, our data  
310 describe a collection of myofibrillar protein kinases and phosphorylation events associated with the z-disc  
311 region that are responsive exercise and warrant further investigation as mediators of exercise-induced cardiac  
312 adaptation.

313 Exercise training has protective effects against cardiomyocyte death and proteins that interact with Bcl-2  
314 family members involved in the regulation of apoptosis and autophagy were enriched amongst the exercise-  
315 responsive phosphoproteome. We discovered new phosphorylation sites (T93 and Y94; Table 1) on Bcl-2  
316 interacting killer-like protein (Bik) which became significantly more phosphorylated 3 h after cessation of  
317 exercise. These sites are different to the previously reported ERK1/2 mediated phosphorylation of Bik at  
318 T124 that is associated with ubiquitination and subsequent degradation of Bik {Lopez 2012} and represent  
319 new targets for further exploration. Phosphorylation of BCL2/adenovirus E1B 19 kDa-interacting protein 3  
320 (BNIP3) was increased after exercise and this protein has been implicated in the regulation of both apoptosis  
321 and mitophagy {Choe 2015} in a manner similar to the better characterised protein Beclin-1 {Maejima 2016}.  
322 In addition, exercise was associated with phosphorylation of Bcl-2-interacting death suppressor (Bag3) on  
323 sites (S176, S277, S278, S377, S387) previously reported in response to beta-adrenergic receptor stimulation  
324 {Lundby 2013}. Bag3 is a co-chaperone of heat shock cognate 70 (hsc70), interacts with heat shock protein  
325 22 and regulates the interaction with poly-glutamate (Poly-Q) proteins which are prone to aggregation.  
326 Phosphorylation of S397 of Bcl-2 associated transcription factor 1 (BCLAF1) increased after cessation of the  
327 exercise (cluster 3) and this protein is required for efficient DNA repair and genome stability {Savage 2014}.  
328 Together our findings describe an unappreciated network of responses in proteins that regulate apoptosis and  
329 autophagy processes, beyond the more widely reported effector proteins such as Bcl-2 and Bax.

330 During exercise myocardial contractility increases to meet the greater demand for cardiac output and this  
331 response is in part driven by  $\beta$ -AR signalling. Approximately one-third (41 of 141 phosphopeptides) of the  
332 exercise-responsive phosphopeptides were previously identified in similar phosphoproteome profiling  
333 {Lundby 2013} of the cardiac response to  $\beta_1$ -AR stimulation, including PKA and archetypal proteins involved  
334 in myocardial contractility/  $Ca^{2+}$ -handling and metabolism. For example, ryanodine receptor phosphorylation  
335 increased during exercise (Figure 4, Cluster 1) and this has previously been associated with augmentation of  
336 intracellular calcium release and enhanced myocardial contractility {Marx 2000}. The SERCA inhibitor,  
337 phospholamban, was phosphorylated at S16, which is noted to be sufficient for a maximal cardiac response to  
338  $\beta$ -AR stimulation {Chu 2000}, and in addition, we report phosphorylation of lesser-known proteins such as  
339 histidine-rich calcium binding protein that also regulates SR calcium release {Arvanitis 2011}. With regard to

340 metabolism, exercise increased S694 phosphorylation of phosphorylase kinase beta (Table 3) which is  
341 responsible for phosphorylation of glycogen phosphorylase and therefore acceleration of glycogenolysis. The  
342 monocarboxylate transporter 1 (Slc161a) was also phosphorylated at a  $\beta_1$ -AR responsive site immediately  
343 after exercise and this may be associated the transport lactate or ketones in to cardiac muscle cells.  
344 Conversely, phosphorylation of the pyruvate dehydrogenase E1 complex subunit alpha (Pdha1) is associated  
345 with inhibition of pyruvate entry to the TCA cycle and was increased 3 h after the cessation of exercise  
346 (Figure 4, Cluster 3) and may be more associated with restoration of cardiac glycogen stores. Notably,  
347 phosphorylation sites reported here in response to exercise and by Lundby et al {Lundby 2013} in response to  
348  $\beta_1$ -AR stimulation do not entirely overlap, and even after taking in to account potential technical differences  
349 between the 2 studies, it is evident that the cardiac exercise response is not entirely driven by  $\beta_1$ -AR  
350 stimulation.

351 Cardiac  $\beta_1$ -AR stimulation is associated with the activation of p38 MAP kinase {Lundby 2013} and this was  
352 also detected in response to exercise (Table 3 and Figure 3A). Previous {Hunter 2008} targeted (western blot)  
353 analysis of signalling proteins in hearts of high- and low-capacity runner rats isolated 10 min after performing  
354 a ramped treadmill test measured a 1.6-fold increase in p38 MAPK (T180/Y182) phosphorylation, which is  
355 corroborated by our data (Figure 3A). We further show Y182-specific phosphorylation of p38 MAPK  
356 (measured by LC-MS; Table S1) is transient and was not significantly different from control 3 h after  
357 exercise. Moreover the change in p38 MAPK phosphorylation clusters with the phosphorylation of proteins  
358 including alpha B-crystallin, heat shock protein 27 and astrocytic phosphoprotein PEA-15 (Figure 4; Cluster  
359 1). Astrocytic phosphoprotein PEA-15 modulates the localisation and activity of ERK 1/2 MAP Kinases  
360 (MAPK1 and MAPK3), phosphorylation of PEA-15 at both S104 and S106 is necessary and sufficient to  
361 prevent its interaction with ERK 1/2 whereas non-phosphorylated PEA-15 blocks the nuclear translocation  
362 and transcriptional capacity of ERK 1/2 {Krueger 2005}. In the current work PEA-15 was phosphorylated at  
363 S104 only, but nonetheless the exercise-responsive phosphoproteome was enriched for proteins involved in  
364 ERK1/2 mitogen-activated protein kinases pathway and approximately 18 % (25 of 141) of the cardiac  
365 phosphorylation sites reported here have previously been identified as ERK1/2 targets by phosphoproteomic  
366 analysis of epithelia cells {Courcelles 2013}.



367 MEK1-ERK1/2 signalling can inhibit Calcineurin-NFAT signalling which is strongly implicated in  
368 pathological cardiac hypertrophy {Molkentin 2004}. Given the large degree of cross-talk between these  
369 pathways more intricate studies are needed to decipher the networks of interactions associated with  
370 pathological versus physiological cardiac adaptations, and the role of currently lesser known components such  
371 as Cyma5 costamere protein, which was phosphorylated in response to exercise, and is a negative regulator of  
372 calcineurin-NFAT signalling cascade {Molkentin 2004} will need to be integrated with the existing canonical  
373 pathways.

374 The IGF-1 receptor/PI3K (p110 $\alpha$ )/ Akt1 pathway is the most thoroughly studied signalling pathway  
375 associated with exercise-induced cardiac adaptation and is associated with Akt S473 phosphorylation {Weeks  
376 2012}. We found no significant change in Akt S473 phosphorylation after an acute bout of treadmill running  
377 which is consistent with previous {Hunter 2008} findings and suggests a single exercise bout is not sufficient  
378 to instigate the IGF-1 receptor signalling in the heart. Nonetheless, acute exercise was associated with  
379 phosphorylation of direct regulators of ribosomal translation such as eukaryotic initiation factors eIF2 and  
380 eIF5. The interaction between eIF-5B and eIF2 $\beta$  is essential for GTP hydrolysis and release of eIF2-GDP  
381 from the 40 S initiation complex and the formation of the 80 S ribosome. Phosphorylation of eIF2 clustered  
382 with ATP-binding cassette sub-family F member 1 (ABCF1) and this interaction (including S109  
383 phosphorylation of ABCF1) has previously been reported to be necessary in both cap-dependent and  
384 independent translation {Paytubi 2009}. Therefore our findings draw attention to regulators of ribosomal  
385 translation initiation that have largely been ignored in previous exercise-related studies.

386 A single bout of exercise can precondition the heart against I/R damage {Frasier 2011} and gap junction  
387 proteins could be a key mechanism underlying this protective effect {Jeyaraman 2012}. Gap junction alpha-1  
388 protein (Cx43) is the main component of gap junctions in the ventricular myocardium and phosphorylation of  
389 S325, S328 and T326 of Cx43 increased 3 h after exercise. Cx43 has a short (<5 h) half-life and  
390 phosphorylation is required for gap junction formation whereas de-phosphorylation is associated with the  
391 disassembly of the gap junction and Cx43 degradation {Solan 2007}. Phosphorylation at 325, 328 and 330  
392 reported here may be mediated by casein kinase 1 {Cooper 2002} or fibroblast growth factor {Sakurai 2013}  
393 and regulate gap junction assembly {Lampe 2006}. In contrast, Cx43 S262 phosphorylation has more

394 commonly been associated with cardiac preconditioning mediated via PKC {Waza 2014} and was not  
395 responsive to exercise. Therefore the current findings highlight a novel exercise-induced mechanism  
396 involving gap-junction assembly/ turnover separate from those involved in ischaemic preconditioning. In  
397 addition, phosphorylation of CX43 co-occurred with the phosphorylation of tight junction protein 2,  
398 Palkophillin-2 and the alpha subunit of the voltage-gated sodium channel (Figure 4, Cluster 3), which have  
399 previously been reported as interaction partners.

400

## 401 **5. Summary**

402 Signal transduction is a dynamic process and we used a time-series design to dissect immediate/early events  
403 such as phospholamban phosphorylation (Figure 4; Cluster 1), which may be more associated with myocardial  
404 contractility, from sustained (Figure 4; Cluster 2) or latter (Figure 4; Cluster 3) phosphorylation events that  
405 may be more associated with the adaptive response to exercise or the restoration of cardiac homeostasis. Non-  
406 targeted analysis detected well established phosphorylation events associated with myocardial contractility  
407 whilst simultaneously detecting new site-specific phosphorylation events on proteins that are not shared with  
408 the cardiac response to  $\beta_1$ -AR stimulation and have not previously been associated with the cardiac exercise  
409 response. In particular, we discovered new phosphorylation sites on 4 cardiac proteins (Table 2), including  
410 S81 of muscle LIM protein, and identified a selection of myofibrillar protein kinases that were also responsive  
411 to exercise and may constitute a putative network of signal transduction for the adaptation to mechanical work  
412 in the heart.

413

414 **Disclosures**

415 None

416 **Funding**

417 This work was supported by Liverpool John Moores University.

418

419 **References**

420 {Bibliography}

421

422 **Table 1 – Physical and physiological characteristics**

	<b>Control</b>	<b>0 h</b>	<b>3 h</b>
Body weight (g)	338 ± 16	350 ± 27	351 ± 9
Heart weight (mg)	1071 ± 44	1005 ± 76	1060 ± 40
VO <sub>2</sub> peak (ml•kg <sup>-1</sup> •min <sup>-1</sup> )		66 ± 5	69.8 ± 5
Peak RER		1.046 ± 0.03	1.021 ± 0.03
Time to completion (min)		21.3 ± 3.6	21.3 ± 3.1

423 Data are presented as Mean ± SD (n = 6, in each group). There were no statistically significant (p<0.05) differences between the groups for any  
 424 of the variables measured.

425

426

427

428

429 **Table 2 – New site-specific phosphorylation sites discovered in cardiac proteins**

Cluster	Protein name	UniProt	Residue	(+/-)7 Sequence
1	Myosin light chain kinase 3	E9PT87	S444	TEAGRRVSpSAAEAAI
2	Obscurin	A0A0G2K8N1	S2974	LGLTSKASpLKDSGEY
3	Cysteine and glycine-rich protein 3	P50463	S81	GQGAGCLSpTDTGEHL
3	Bcl2-interacting killer-like protein	Q925D2	T93 & Y94	MHRLAATpYpSQTGVR

430

431

432

433

**Table 3 – Phosphorylated kinase enzymes**

Cluster	Protein name	UniProt	Residue
1	Myosin light chain kinase 3	E9PT87	S444
1	p38 mitogen-activated protein kinase	Q56A33	Y182
1	Phosphorylase kinase beta	Q5RKH5	S694
1	Titin	Q9JHQ1	S402
1	Titin	Q9JHQ1	S1990
2	cAMP-dependent protein kinase	P09456	S77 & S83
2	Obscurin	A0A0G2K8N1	S2974
2	Striated muscle specific serine/threonine kinase	Q63638	S2410 & S2414
2	Titin	Q9JHQ1	S256 & T267
2	Titin	Q9JHQ1	S32863
3	cAMP-dependent protein kinase	P09456	S83
3	Titin	Q9JHQ1	T300 & S302
3	Titin	Q9JHQ1	S1332 & S1336

435

436

437

438

439

440 **Figure Legends**

441 **Figure 1 - Measurement of VO<sub>2</sub>peak**

442 Example oxygen uptake (VO<sub>2</sub>) and carbon dioxide production (VCO<sub>2</sub>) traces during an incremental  
443 exercise test designed to elicit peak oxygen uptake (VO<sub>2</sub>peak).

444

445 **Figure 2 - Changes in the abundance of exercise responsive phosphopeptides**

446 Volcano plots presenting the distribution of the fold-change (log<sub>2</sub>) in abundance and statistical  
447 significance of phosphorylated peptides. Post-hoc comparisons are shown for (A) non-exercised  
448 control hearts vs hearts isolated immediately (0 h) after cessation of the graded exercise test, or (B)  
449 non-exercised control hearts vs hearts isolated 3 h after cessation of the graded exercise test.

450

451 **Figure 3 – Exercise responsive phosphorylation of cardiac p38 MAPK and CRYAB**

452 Western blot analysis of the ratio of phosphorylated: non-phosphorylated p38 mitogen activated  
453 kinase (p38 MAPK; A) and alpha B crystallin (CRYAB; B). Cropped images of 3 representative lanes  
454 from a single animal from the control, 0 h and 3 h groups are shown. Data are presented as mean ±  
455 SEM (*n* = 6, per group) and statistical significance (\**P*<0.05 different from control group) was  
456 determined by one-way analysis of variance and Tukey HSD post-hoc analysis.

457

458 **Figure 4 – Hierarchical clustering of exercise responsive phosphopeptides**

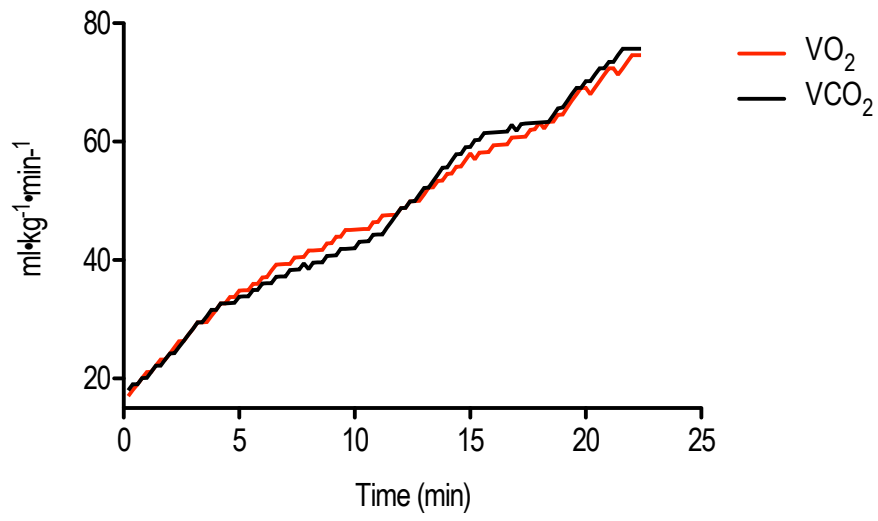
459 Unsupervised hierarchical clustering was performed on 141 phosphopeptides that exhibited statistically  
460 significant (*P*<0.05) differences across time by one-way ANAVO. Known and predicted interactions  
461 between proteins within each cluster were then investigated using the Search Tool for the Retrieval of  
462 Interacting Genes/Proteins (STRING). (A) **Cluster 1** contains phosphopeptides whose abundance  
463 significantly increased immediately after exercise and then returned to basal levels within 3 h after  
464 cessation of the exercise test; this cluster included phosphorylation of phospholamban (Pln) and a  
465 network of p38α (MAPK14) stress-responsive proteins including alpha B-crystallin (Cryab) and heat



466 shock 27 kDa protein (Hspb1). (B) **Cluster 2** contains phosphopeptides whose abundance increased  
467 immediately after exercise and further increased 3 h after cessation of the exercise test; this cluster  
468 included phosphorylation of costamere and gap junction proteins such as vincullin and connexin 43  
469 (Gja1). In addition, ribosomal proteins, such as eukaryotic initiation factor 2 (eIF2s2) and ATP  
470 binding cassette sub-family F member 1 (Abcf1), which regulate both cap-dependent and independent  
471 translation were phosphorylated in response to exercise. (C) **Cluster 3** contains phosphopeptides  
472 whose abundance decreased immediately after exercise and then returned to basal levels within 3 h  
473 after cessation of the exercise test; this cluster included phosphorylation of myofibrillar proteins,  
474 including muscle LIM protein (Csrp3).

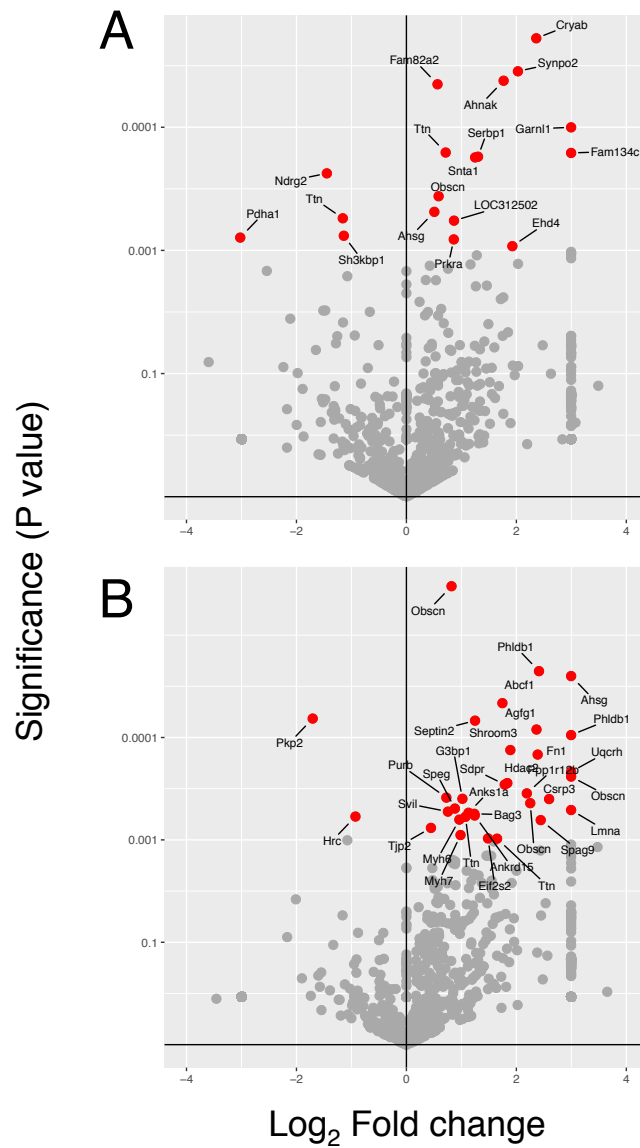
475

476 **Figure 1**

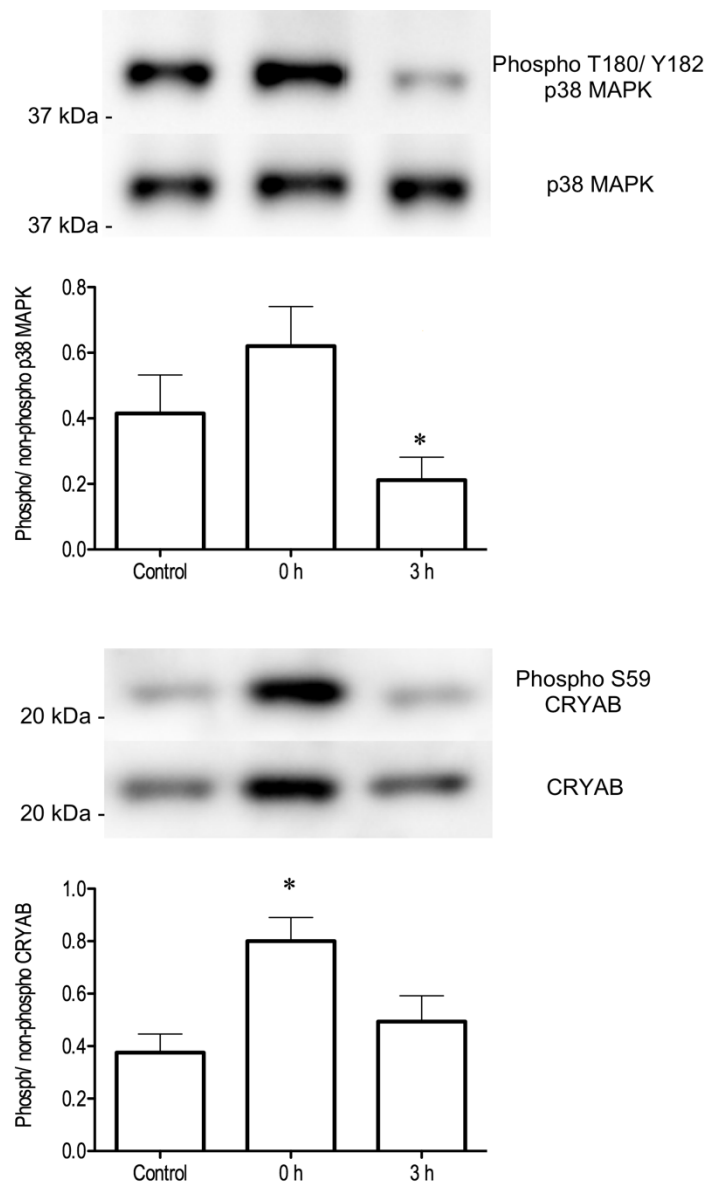


477

478

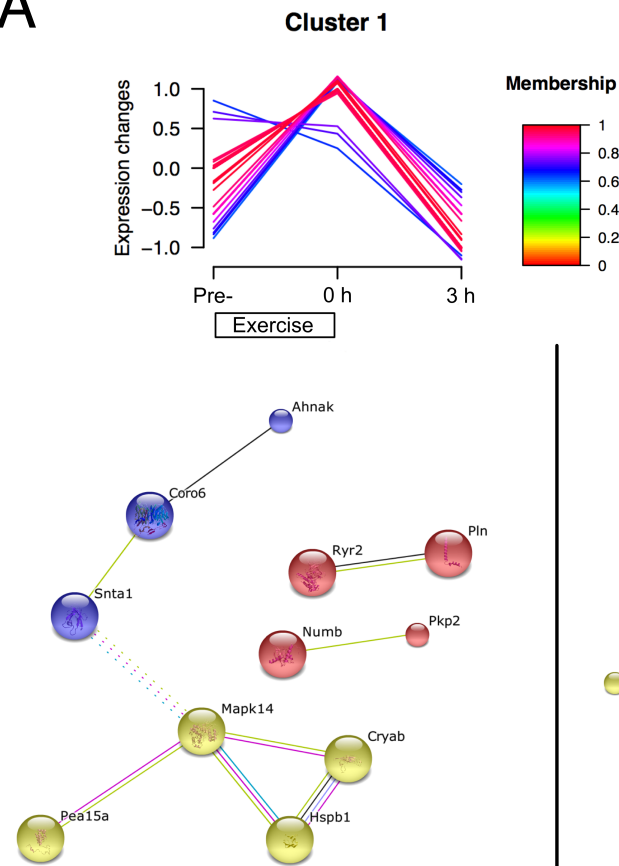


483 **Figure 3**

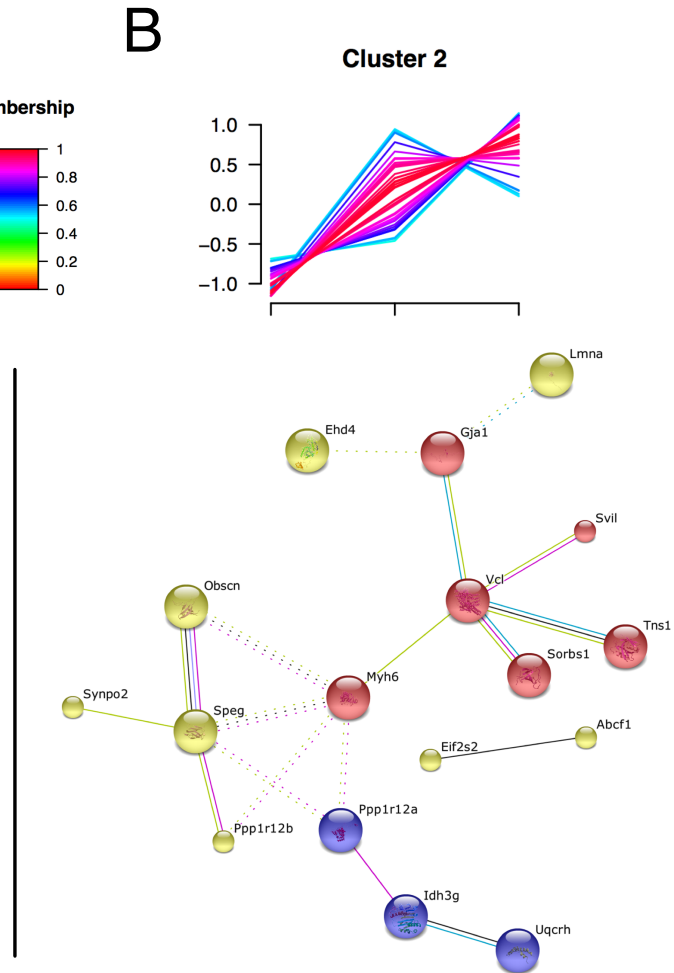


484  
485

**A**



**B**



**C**

